Water Resources Research

RESEARCH ARTICLE
10.1029/2019WR026751

The Drivers of River Temperatures Below a Large Dam

Miles E. Daniels[1] and **Eric M. Danner**[2]

[1]University of California, Santa Cruz, Institute of Marine Sciences, Affiliated with: Fisheries Ecology Division, Southwest Fisheries Science Center, National Marine Fisheries Service, National Oceanic and Atmospheric Administration, Santa Cruz, CA, USA, [2]Fisheries Ecology Division, Southwest Fisheries Science Center,National Marine Fisheries Service, National Oceanic and Atmospheric Administration, La Jolla, CA, USA

Key Points:
- Dam discharge temperature, air temperature, and solar radiation were the primary drivers of river temperature
- River temperature drivers varied spatially; dam discharge temperature drove upstream reaches and air temperature drove downstream reaches
- Dam discharge temperature was often a larger driver of downstream river temperature compared to discharge volume

Supporting Information:
- Supporting Information S1

Correspondence to:
M. E. Daniels,
miles.daniels@ucsc.edu

Citation:
Daniels, M. E., & Danner, E. M. (2020). The drivers of river temperatures below a large dam. *Water Resources Research*, *56*, e2019WR026751. https://doi.org/10.1029/2019WR026751

Received 12 NOV 2019
Accepted 26 MAR 2020
Accepted article online 4 APR 2020

Abstract Temperature is a fundamental aspect of water quality in rivers, controlling the rate of many ecological processes. By disrupting the flow of water, large reservoirs and dams can fundamentally alter downstream temperature regimes by resetting the water temperature and flow boundary conditions at the dam release point. Therefore, it is critically important to understand how the volume and temperature of these releases interact with meteorological conditions to influence downstream temperature dynamics. In this study, we modeled temperature dynamics in a large regulated river (Sacramento River, CA, USA) to better understand how heat fluxes, and ultimately river temperatures, responded to different physical drivers connected to meteorology and the upstream boundary conditions established by dam operations. We used a quantitative process-based model of river temperature (RAFT), combined with sensitivity analysis, to identify the dominant physical drivers of temperature in the Sacramento River, and explored how these drivers varied over space and time. The physical drivers that had the greatest influence on temperature dynamics were dam discharge temperature, air temperature, and solar radiation. The primary controlling factors were dam discharge temperature in the most upstream reaches and air temperature in the most downstream reaches. When isolating the effect of boundary conditions on downstream river temperature, we observed that temperatures closer to the dam under all but low flow conditions responded more to changes in dam discharge temperature than dam discharge volume. Understanding the spatial and temporal extents of drivers of heat flux and their relative importance is critical when managing for river temperature.

1. Introduction

River temperatures can be highly dynamic in space and time, and the downstream transport and transformation of heat are fundamental processes which shape biological (Angilletta & Angilletta, 2009; Martins et al., 2011), chemical (Boulêtreau et al., 2012; Demars et al., 2011), and physical characteristics of fluvial systems (Costard et al., 2003). Temperature is an expression of the average heat content of a material, and the primary external factors thought to determine the temperature for a given length of river are lateral inputs of heat (e.g., tributaries), heat exchanges at the air-water surface interface (e.g., air temperature and evaporation), and heat exchanges at the bed-water interface (e.g., groundwater inputs) (Caissie, 2006; Poole & Berman, 2001). Because the transport of heat downstream is primarily driven by advection, and to a lesser extent dispersion, the response of river temperature to these heat fluxes (i.e., changes in heat/temperature over time) is also heavily influenced by the starting upstream temperature (boundary condition) (Poole & Berman, 2001). Dams effectively reset this boundary condition by impounding water and creating a buffer in heat exchange, altering the natural downstream hydrograph and thermograph (Cai et al., 2018; Niemeyer et al., 2018; Preece & Jones, 2002). As a result, dam operations can have a strong influence on the temperature landscape downstream, especially when they are managed with the goals of achieving specific temperature targets (Olden & Naiman, 2010).

Because of the importance of river temperature in aquatic ecosystems, it is critical to understand how releases from reservoirs and dams interact with the dominant drivers of heat flux in rivers to impact temperatures downstream. This can be done using simulation models of heat fluxes and river temperature to evaluate the relative contributions of the primary drivers under past, current, and future conditions (Cai et al., 2018; Garner et al., 2017; Webb & Zhang, 1997; Wondzell et al., 2019). We used sensitivity analysis, where model inputs (e.g., meteorological and hydrological), which force heat flux are perturbed to

evaluate the magnitude of change in model output (i.e., river temperature). The perturbed model inputs associated with the largest magnitude change in model output are then interpreted as the driving term(s) behind heat flux for a given river location and time (Saltelli et al., 2008). Additionally, using process-based river temperature models for such sensitivity analysis allows for causal inference, as opposed to using sensitivity analysis with a statistically based model, where the relationships between inputs and outputs are not mechanistic. Simulation models can also be used to explore how changing boundary conditions (e.g., dam discharge volume and temperature) will impact the magnitude and spatial extent of changes in river temperature downstream.

Our objectives for this study were to (1) characterize the spatial and temporal variation of heat flux in a regulated river where temperature is, in part, managed to meet ecological goals, (2) identify which physical drivers were most responsible for this flux (i.e., water temperature change), and (3) examine the role of upstream boundary conditions on influencing downstream river temperatures. We applied this approach in a case study of the Sacramento River in California's Central Valley, a large regulated river in a Mediterranean climate. We first used a mechanistic river temperature model (Pike et al., 2013) to reconstruct the subhourly temperature regime of 340 km of the Sacramento River over a 28-year period (1990–2017). This allowed us to better understand the temporal and spatial trends and ranges of heat fluxes. We then conducted global sensitivity analysis, parameterized from the retrospective analysis, to identify dominant physical drivers of river temperature change in the system. Last, we ran a suite of scenarios perturbing dam discharge volume and temperature to identify the spatial and temporal extent of the downstream river temperature response to these boundary conditions.

2. Methods

2.1. Study Site

Sacramento River is the largest river in California, draining an area of approximately 7 million hectares or 17% of California's total surface area. The river terminates at the Sacramento-San Joaquin Delta about 750 km from its headwaters. The Delta connects to the Pacific Ocean through San Francisco Bay. The majority of the Sacramento River is located in California's Central Valley, a low-relief region that is characterized by a combination of volcanic and alluvial material. Since the mid-1900s, the mainstem of the Sacramento River has been regulated by two dams in the upper portion of the watershed: Shasta and Keswick. Shasta Dam is upstream of the Central Valley and impounds the largest reservoir in the state by volume (Shasta Reservoir), at approximately 5.6×10^9 m^3. Keswick Dam is a short distance downstream, forms the after bay of Shasta Dam (Keswick Reservoir), has much less storage capacity (2.7×10^7 m^3), and is primarily used to stabilize discharge from Shasta power peaking. Downstream from Shasta and Keswick to the Delta, there are numerous tributary inputs (regulated and unregulated), which contribute to hydraulic and heat loadings to the mainstem in addition to water diversions for municipal, industrial, and commercial uses.

2.2. River Temperature Model

We used a one-dimensional river temperature model, RAFT (Pike et al., 2013), to simulate temperature dynamics of the Sacramento River below Keswick Dam. The domain of the model is from Keswick Dam to 340 km downstream near the city of Sacramento, just prior to the confluence of the Feather River (Figure 1). The model simulates spatially explicit heat exchange processes in the longitudinal (i.e., downstream) direction and assumes homogenous lateral and vertical temperature within each segment of river channel. We ran simulations at a spatial resolution of 2 km and a temporal resolution of 10 min to adequately capture the scale at which temperature dynamics occurred and to ensure numeric stability (Chapra, 2008). In addition to the upstream boundary inputs (Keswick Dam discharge and temperature), the model structure accounts for the hydraulic and heat loadings from six primary tributaries entering the system. The model uses meteorology (solar radiation, air temperature, relative humidity, and wind speed) as air-water interface forcing terms. Heat flux between the water and channel bed are also simulated via a simple model of conduction after initialized with the temperature of overlaying water. Further details, including calibrated values of parameter values, of the RAFT model can be found in Pike et al. (2013), but the primary equation used to account for how different sources of heat enter and exit the river over space (x) and time (t) is described by

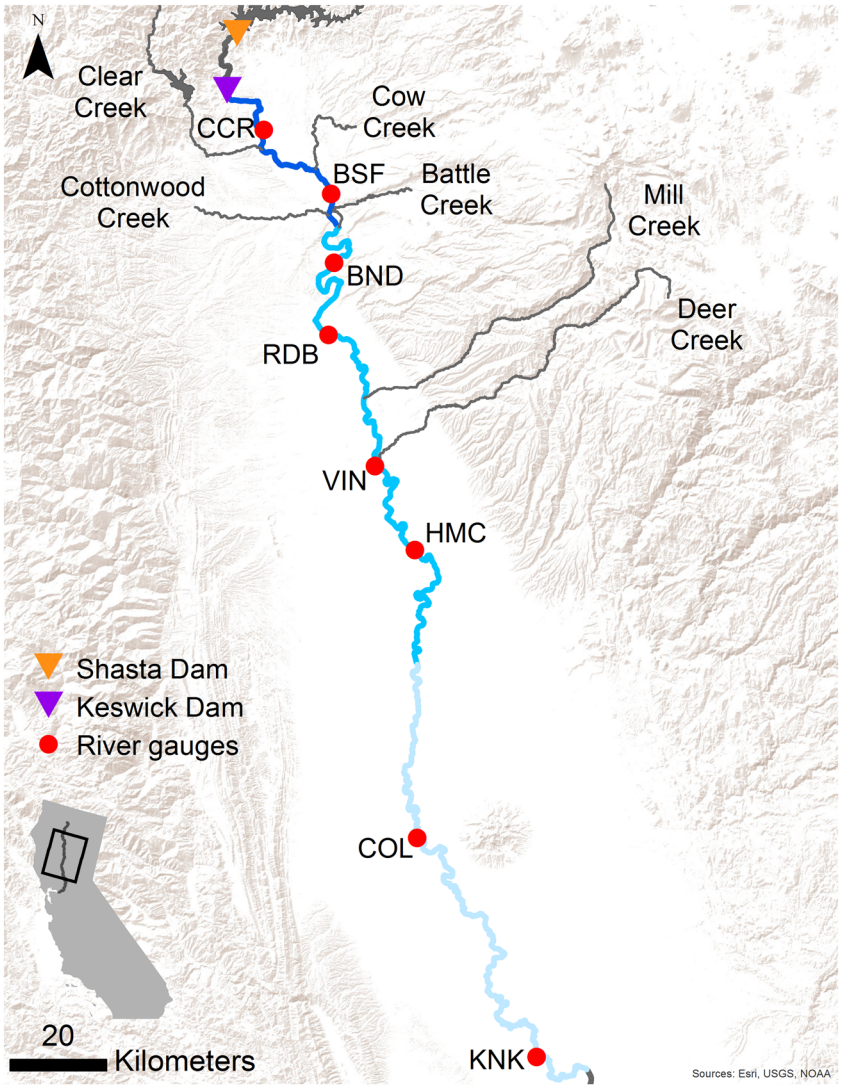

Figure 1. Map of RAFT model domain showing locations for Shasta and Keswick dams, river temperature gauges, and tributary inputs. Note: There is a temperature gauge just downstream from Keswick Dam.

$$\frac{\partial T}{\partial t} = -U \cdot \frac{\partial T}{\partial x} + D \cdot \frac{\partial^2 T}{\partial x^2} + \frac{\Phi_{sol} + \Phi_{atm} + \Phi_{wat} + \Phi_{lat} + \Phi_{Sen} + \Phi_{bed}}{\rho C_p \overline{d}} \quad (1)$$

where $\frac{\partial T}{\partial t}$ is change in river temperature (T; °C) over time (s); U is the channel advection rate (m s^{-1}); D is the longitudinal dispersion rate (m^2 s^{-1}); Φ identifies individual heat fluxes (W m^{-2}) including downward shortwave radiation (*sol*), incoming longwave radiation (*atm*), outgoing longwave radiation (wat), latent heat of evaporation (*lat*), conduction (*sen*), and streambed conduction (*bed*); ρ is density of water (kg m^{-3}); C_p is specific heat of water (J (kg °C)$^{-1}$); and $\overline{d}$ is channel mean water depth (m).

2.3. Retrospective Analysis

To better understand temporal and spatial trends of heat fluxes along the Sacramento River, and to help parameterize global sensitivity analyses (GSA), we used RAFT to reconstruct the temperature regime of the Sacramento River from 1990 to 2017. To improve the ability to reconstruct historic river temperatures, we used a version of the Ensemble Kalman Filter (Evensen, 2009; Pike et al., 2013) data assimilation technique and updated the model state variables of river temperature using information (i.e., recorded temperatures) from mainstem gauge sites at each time step. For model inputs, observed discharge and temperature

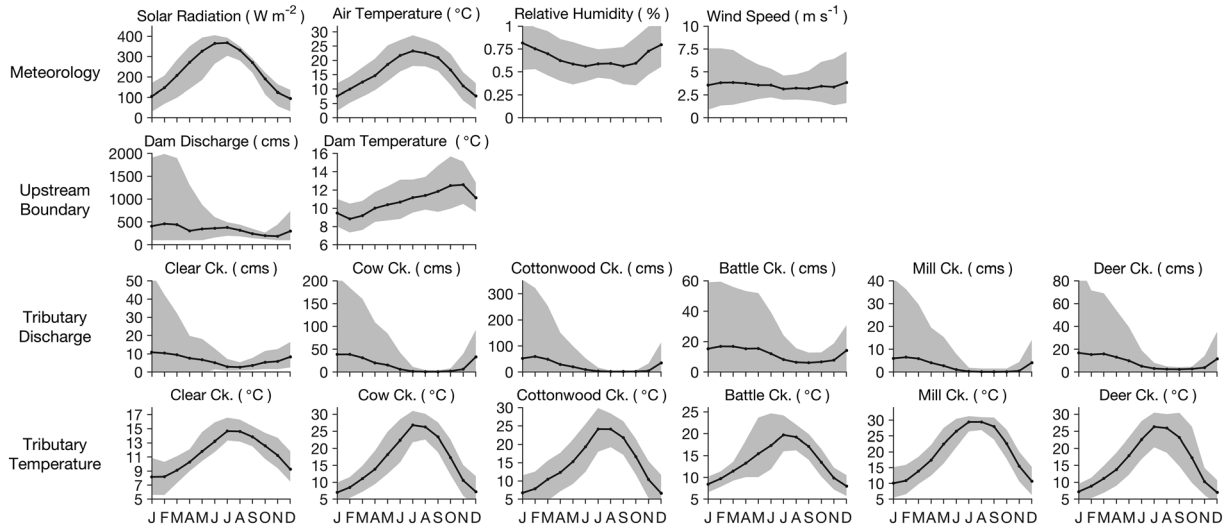

Figure 2. Model inputs perturbed in global sensitivity analysis. Panels show historical monthly means (black line) and ranges (shaded region) estimated for 1990–2017 from sources identified in the text.

from upstream (i.e., Keswick Dam) and lateral (tributaries) gauges were gathered from federal and state agencies (CDEC, USGS, and CA-DWR), filtered, and gap filled (Elsner & Tsonis, 2013; Toffolon & Piccolroaz, 2015). Meteorological forcing terms were gathered from the North American Regional Reanalysis (NARR, 2004). The North American Regional Reanalysis is a gridded weather dataset consisting of a 32 km, 3-hourly, data-assimilated hindcast that we bias corrected using empirical quantile mapping (Chen et al., 2013).

2.4. Global Sensitivity Analysis

To quantify the relative contributions of the various physical drivers of river temperature, we conducted a series of GSA using RAFT with previously calibrated parameter values (Pike et al., 2013). Detailed descriptions of the methods and purposes of GSA can be found elsewhere (Pianosi et al., 2016), but a primary goal of GSA is to identify which model inputs are associated with the greatest variability in a model's output. This is done by perturbing multiple model inputs repeatedly over a user defined parameter space. The relationship between perturbed inputs and model output is then estimated by calculating a sensitivity index for each input examined. The formula for a sensitivity index is specific to the type of GSA performed and is used to infer which inputs are driving model output by quantitative ranking or some other means.

The output of any GSA is strongly dependent on the input parameter space being explored (Saltelli et al., 2008), and it is therefore critical to define the range of input values based on the questions/hypotheses driving the analysis. To define our parameter space and ensure that feasible ranges were selected, we used information gained from the retrospective analysis and identified minimum and maximum values of RAFT inputs on a monthly time scale. Thus, our GSA is bounded by the range of monthly historical variability in meteorology, hydrology, and dam operations. We selected 18 model inputs to be evaluated with GSA in regards to their effect on river temperature (Figure 2). These were grouped into meteorological forcing terms, upstream boundary conditions, and lateral tributary inputs of discharge volume and temperature.

RAFT is a spatially and temporally explicit model, which can complicate the interpretation of the GSA output. For example, because the water from a perturbed upstream input, such as dam discharge volume, at time T_1 does not arrive at a downstream location (L_2) until a later time (T_2), calculating a sensitivity index for location L_2 at time T_1 from the dam perturbation at T_1 would not be appropriate. To simplify this complexity and remove travel- and/or lag time effects, we ran RAFT under a press disturbance fashion until the system reached longitudinal temperature equilibrium. Longitudinal temperature equilibrium was defined as the most downstream model segment maintaining a constant daily average river temperature for more than 2 days. To run RAFT under a press disturbance, we held all inputs constant in regards to a daily mean value

sampled from the historical monthly ranges shown in Figure 2, while retaining subdaily/diel variability in meteorological inputs such as air temperature. An example and additional details of this approach can be found in supporting information section S1.

The computational cost of GSA increases with additional inputs examined; therefore, we first applied a computationally efficient screening (or factor fixing) GSA to identify model inputs with low sensitivity. We then used fixed values (i.e., historical monthly means; see from Figure 2) for these low sensitivity inputs in subsequent analyses. The screening used the elementary effects test (EET; Morris, 1991; Saltelli et al., 2008). EET is referred to as a one-at-a-time method, where during each model simulation a single input is perturbed and all others held constant. This occurs sequentially over 'M' inputs and is repeated "r" times for each input, such that the total number of simulations is $N = r \cdot (M+1)$. All input values (both those held constant and varied) are random samples from a defined parameter space. The EET sensitivity indices used for inference are the absolute means ($^*\mu$) and standard deviations (σ) (Campolongo et al., 2007). The absolute mean represents the magnitude of model sensitivity to a single input across the range of all other inputs examined and the standard deviation represents the degree that an input's magnitude is conditional on another input (i.e., interaction). Larger relative values of $^*\mu$ represents greater model sensitivity to a given input. As we were interested in how the physical drivers of river temperature vary with time, we conducted separate EET analyses for each month, with each month for each input composed of 500 simulations (i.e., EET parameter $r = 500$) using a Latin Hypercube sampling strategy (Saltelli et al., 2008). We used these monthly sensitivity indices (scaled between 0 and 1) as the primary metrics for screening, such that inputs in the lower 10th percentile of either μ^* or σ distributions for a given month across the entire river study domain were dropped from further analysis (see supporting information section S2 for an example).

For the inputs retained after the screening analysis, we used a ranking GSA to identify inputs associated with the largest change in model output (i.e., drivers of river temperature). This was done using a density-based approach, known as the PAWN method described by Pianosi and Wagener (2015). PAWN works by comparing the empirical cumulative distribution function (CDF) of simulated river temperatures that are conditional (N_c) versus unconditional (N_u) on perturbed inputs. Unconditional CDFs use all-at-a-time sampling (Pianosi et al., 2016) of inputs, so that each simulation has a different random, Latin Hypercube derived, set of inputs (i.e., not conditional on specific input values). Conditional CDFs hold a single parameter constant, varying the constant randomly over n simulations, while all other parameters are also sampled randomly as in the unconditional case. The value of the two-sample Kolmogorov-Smirnov test (Hogg et al., 1977), comparing the unconditional and conditional CDFs for each input, is then used as the sensitivity index. The PAWN sensitivity index ranges from 0–1, with a larger value indicating greater divergence of the conditional CDF from the unconditional CDF and therefore greater model sensitivity to that input parameter. The total number of simulations used to calculate the sensitivity index for M inputs is $N = N_u + n \times N_c \times M$. We generated unconditional CDFs from 5,000 model simulations (i.e., PAWN parameter $N_u = 5{,}000$), and we generated conditional CDFs from 125,000 model simulations (i.e., PAWM parameters $N_c = 200$ and $n = 50$) by perturbing $M = 12$ model inputs. As with EET, we ran separate analyses on a monthly basis to identify temporal trends and also ran analyses at specific RAFT model segments to explore potential spatial trends in drivers of river temperature.

2.5. Upstream Boundary Conditions

To explore the sensitivity of river temperature to upstream boundary conditions, we ran a suite of simulations where we perturbed dam discharge volume and/or temperature and evaluated the downstream river temperature response. Simulations occurred for each month of the year and we based the range of perturbations on historical conditions during the retrospective modeling period (1990–2017). These monthly simulations were subsequently aggregated to river temperature cooling (i.e., temperatures cooled in a downstream direction; November–January) and warming (i.e., temperatures warmed in a downstream direction; February–October) periods for summary purposes. Thus, the analysis was set in the context of monthly historic variability of dam operations. Annual discharge volume ranged from 100 to 2,000 cubic meters per second (cms), while discharge temperature ranged from 7 to 16 °C.

Simulations for each month consisted of generating a pair of dam discharge volume and temperature values, which were the historical monthly mean values (see Figure 2). We then perturbed these inputs at increments of ±0.1 standard deviations from the mean (i.e., 0.1 Z-score adjustments) within the range of historical

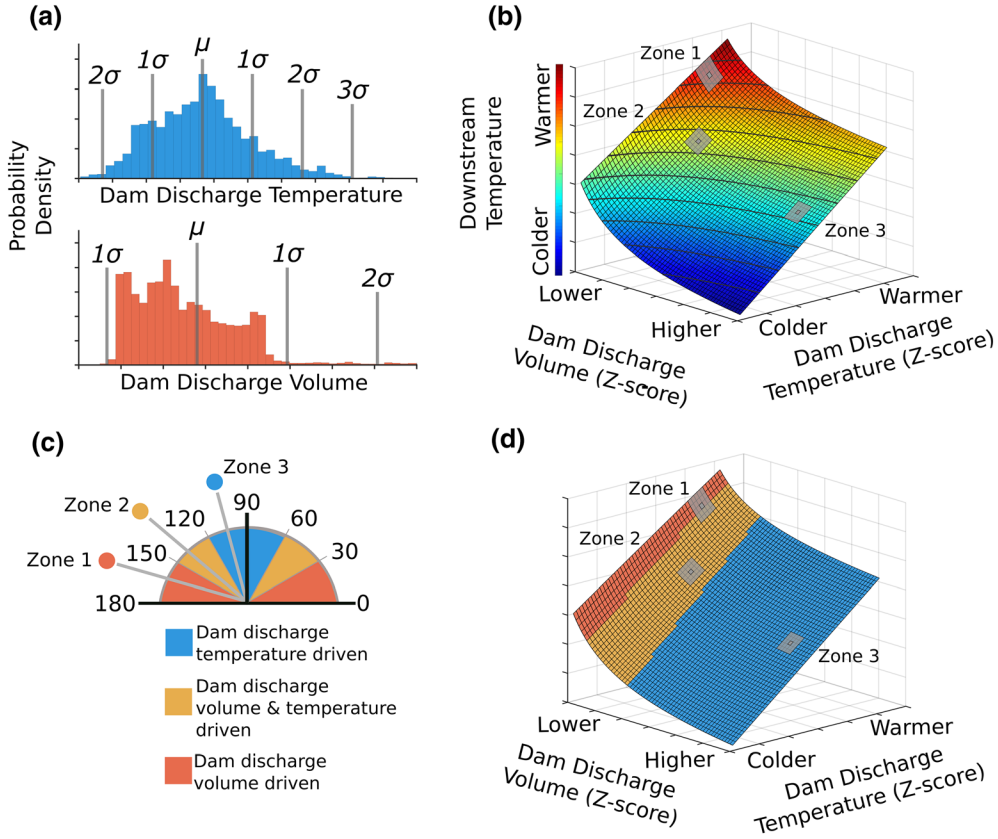

Figure 3. Graphical representation of the gradient approach used to infer under what conditions river water temperature responds more to changes in upstream dam discharge volume or temperature. (a) Example of determining units to change dam discharge temperature and volume based on the Z-score of historic variability, where one Z-score is one standard deviation (σ) from the mean (μ). (b) Relationship between discharge temperature (X axis), discharge volume (Y axis), and downstream temperature (Z axis), with three zones called out to highlight the gradient approach. (c) Classification scheme to identify primary drivers of river temperature based on the angle of steepest gradient in the river temperature response surface over a 4 × 4 window, where the direction of the angle is in reference to the dam discharge volume axis in (b) (i.e., Y axis) for an origin at the center of a 4 × 4 window (i.e., pair of dam discharge volume and temperature), with examples from three zones displayed. (d) Result from classifying entire river temperature response surface shown in (b) as primarily driven by dam temperature (blue dot), volume (red dot), or a combination of temperature and volume (orange dot).

variability for a given month (Figure 3a). To aggregate the monthly results into two primary time periods, that is, when the river is in a cooling period versus a warming period, we conducted the same analysis as done for individual months but perturbed inputs based on the cooling/warming period mean (e.g., for the cooling period from November to January the historical mean was based on these 3 months). We fixed all other inputs (tributary temperature and discharge and meteorology) in the model at mean monthly/period values to better isolate the effect of dam discharge volume and temperature, while incorporating diel variability in the meteorology parameters, such as air temperature. This resulted in a river temperature response surface for the dam discharge volume and temperature pairs evaluated (Figure 3b).

To quantify the effect of dam discharge volume and temperature on downstream river temperature, we used a gradient approach. On the river temperature response surface (Figure 3b), we calculated the angle of the steepest gradient (i.e., largest change in water temperature, max∇) from an origin that was defined by a given dam discharge volume and temperature pair. The direction of the angle of steepest gradient was in reference to the Y axis (i.e., dam discharge volume on Figures 3b and 3d), such that conditions diverting from that axis corresponded to river temperature responding more to dam discharge temperature compared to discharge volume. The search area for calculating the steepest gradient at each pair was a 4 × 4 window

Table 1
Error Statistics (°C) With Mean (Min-Max) for Retrospective Analysis From 1990–2017 for Eight Water Temperature Gauging Stations on the Sacramento River Shown in Figure 1, Calculated From Daily Averages

Gauge	Distance from Keswick (km)	Root mean square error	Mean absolute error	Bias
CCR	14	0.18 (0.10, 0.29)	0.14 (0.07, 0.21)	−0.09 (−1.12, 0.06)
BSF	41	0.45 (0.27, 0.79)	0.35 (0.22, 0.63)	0.08 (−0.35,0.39)
BND	72	0.32 (0.18, 0.66)	0.25 (0.14, 0.58)	0.07 (−0.18, 0.55)
RDB	94	0.3 (0.21,0.79)	0.28 (0.17, 0.64)	0.11 (−0.12, 0.59)
VIN	134	0.63 (0.47,0.86)	0.52 (0.40, 0.69)	0.30 (−0.58, 1.14)
HMC	164	0.40 (0.35,0.46)	0.32 (0.28, 0.37)	−0.44 (−1.06, 0.06)
COL	250	0.44 (0.37, 0.51)	0.35 (0.30, 0.40)	−0.17 (−0.78, 0.10)
KNK	338	0.43 (0.29,0.98)	0.34 (0.23, 0.75)	−0.01 (−0.64, 0.23)

centered on the pair/origin (i.e., searching over a 0.4 × 0.4 Z-scores). Thus, the steepest gradient corresponded to the larger river temperature response per unit of historical variability in dam discharge temperature and volume. This gradient approach allowed us to categorize when river temperature was driven more by discharge volume, temperature, or by a combination both (Figures 3c and 3d).

3. Results

3.1. Retrospective Analysis

Model reconstructions of the temperature regimes of the Sacramento River from 1990 to 2017 generally predicted daily average water temperature within 0.5 °C of observed values (Table 1 and supporting information Figure S4). Error varied over the model domain but tended to increase with distance downstream from the upstream boundary condition at Keswick Dam. Model predictions were evenly positively and negatively biased (i.e., at four out of the eight gauging stations). Other river temperature models have reported error statistics within similar ranges (i.e., <2 °C for root-mean-square and mean absolute error; Norton & Bradford, 2009; Null et al., 2010; Yearsley, 2012).

River temperatures showed consistent spatial and temporal trends over the simulation period (1990–2017). Using correlation analysis on daily mean river temperatures, we characterized the river into three distinct reaches that reflected the influences from upstream dam releases (obtained from a gauge just below Keswick Dam) and meteorological forcing, (Figure 4). Reach-1 was highly correlated ($\rho = 0.96$) with dam discharge temperature, Reach-2 was identified as a transition zone where river temperatures were correlated with both dam release (water) and air temperature, while Reach-3 was highly correlated with air temperature ($\rho = 0.93$). Temporally, the annual mean temperature and range (maximum daily to minimum daily) was reach dependent, with both metrics increasing from Reach-1 to Reach-3. Annual mean temperatures in Reach-1, Reach-2, and Reach-3 were 11, 13, and 15 °C respectively, while annual ranges were 4, 8, and 13 °C respectively. Overall, the spatial and temporal trends of river temperature tended to mimic either dam release temperature, air temperature, or an interaction of the two.

Heat flux (°C Δ day^{-1}) was spatially and temporally variable over the simulation period (Figure 5). There was a consistent spatial trend of decreasing flux from upstream to downstream, often with more than twice as much flux occurring in Reach-1 compared to Reach-3 for each individual component of the total flux (blue vs. orange symbols in Figure 5). There was a temporal trend with the greatest flux occurring in the summer period for all reaches. The highest seasonal variation in flux occurred in Reach-1 and decreased downstream. Advection-dispersion and meteorological fluxes contributed to the greatest change in river temperature (frequently >2 °C day^{-1}), with much smaller contributions from tributary and the channel bed flux (frequently <1 °C day^{-1}). Advection-dispersion fluxes were highly negative for the majority of time as colder water was transported from upstream to downstream at high rates (i.e., river velocity was high and water warmed as it moved in a downstream direction). Tributary fluxes were more notable in Reach-1 compared to Reach-2, where Reach-1 and 2 contain four and two tributaries respectively, with the difference between tributary and mainstem temperature greater in Reach-1 compared to Reach-2 (see Figures 2 and 4). Tributary fluxes were non-existent in Reach-3 as no tributary inputs were simulated. For similar plots of the primary heat terms of equation 1, see supporting information Figure S6.

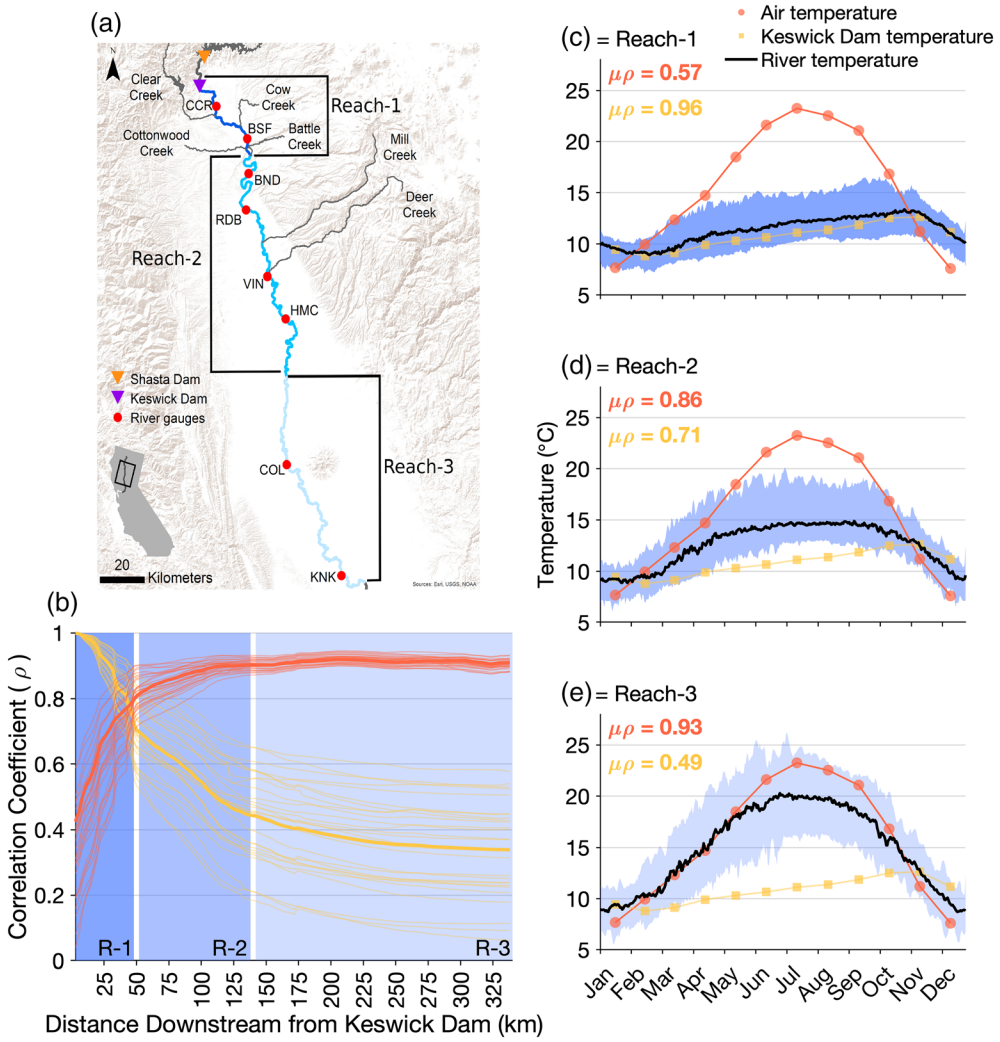

Figure 4. Classification of Sacramento River into three reaches with varying levels of correlation between dam discharge temperature (yellow) and air temperature (red). (a) Map of the three reaches. (b) Correlation between mean daily river temperature, dam discharge temperature, and air temperature from 1990–2017, with mean relationship for all years (bold a line for each respective color). (c–e) Temporal relationship between mean daily river temperature, dam discharge temperature, and air temperature for the three river reaches.

3.2. Global Sensitivity Analysis

Over the entire model domain, simulations of river temperature were most sensitive to meteorological and dam inputs and less sensitive to tributary inputs, as determined by scaled results from the screening analysis (i.e., the EET, Figure 6), with 12 total inputs retained for further sensitivity analysis. Air temperature and solar radiation were the most sensitive across the majority of months (higher $*\mu$) and also had a medium/high level of interaction with other inputs as indicated by the standard deviation of the sensitivity index (σ EE). The boundary condition of Keswick Dam discharge temperature was moderately sensitive across all months but had a low level of interaction with other inputs. The majority of tributary flow and temperature inputs in most months had a negligible effect on river temperature, with the exception of Cow, Cottonwood, and Battle creeks. All three of these tributaries discharge water into Reach-1 at temperatures warmer than the mainstem for the majority of time.

Of the drivers of river temperature selected from the screening process (all meteorology inputs, upstream discharge volume and temperature, and tributary discharge volume and temperature from Cow, Cottonwood, and Battle creeks), the effects of some were more variable over space than over time, while others showed

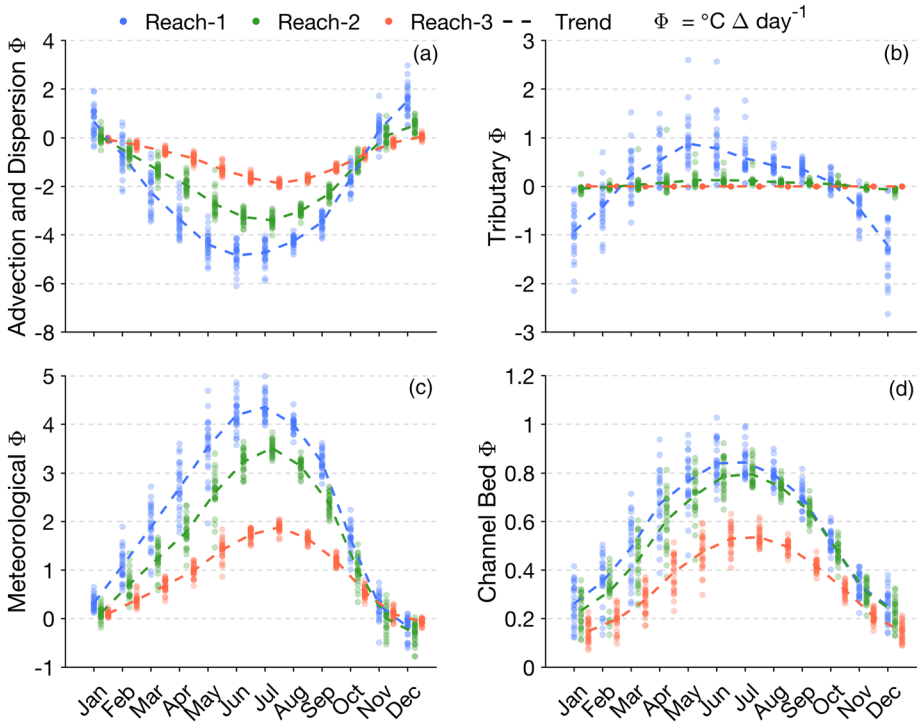

Figure 5. Mean monthly heat flux (Φ = °C Δ day^{-1}) trends for Reach-1 (blue dot), Reach-2 (green dot), and Reach-3 (orange dot) on the Sacramento River from 1990–2017 for the primary fluxes simulated in the retrospective analysis. A dashed line connecting mean monthly values for each reach highlights general seasonal trends. Positive heat flux values represent sources adding heat to the river, while negative values represent sources contributing to removing heat from the river.

similar variability in both space and time (PAWN GSA stratified by river reach and month, Figure 7). Solar radiation (Figure 7a) had the lowest sensitivity near the upstream boundary (Reach-1) and the highest sensitivity near the downstream boundary (Reach-3). The temporal variation in sensitivity to solar radiation also increased from upstream to downstream with sensitivity being highest during winter/spring months and lowest during summer/fall months, corresponding to the historical variability observed in Figure 2. Sensitivity to air temperature (Figure 7b) increased as distance from the upstream boundary increased, with sensitivity being greatest during the summer months when historical air temperatures are the warmest (Figure 2). River temperature sensitivity to relative humidity and wind speed (Figures 7c and 7d) also increased in downstream directions, with sensitivity being lowest during summer and greatest during winter. For upstream boundary conditions, sensitivity to dam discharge volume (Figure 7e) increased in a downstream direction, with temporal sensitivity being greatest near the transition from winter to spring, when flows tend to be highest. Dam discharge temperature sensitivity was greatest in Reach-1 and declined in Reach-2 and Reach-3 (Figure 7f), while there was little variation in sensitivity across months for a given reach as indicated by the nearly linear polynomial fit. Grouping tributary inputs of discharge volume and temperature showed the lowest level of sensitivity in both space and time (Figures 7g and 7h). Most drivers had some level of spatial variability, and some (solar radiation, air temperature, and reservoir discharge volume) also had clear levels of temporal variability.

3.3. Upstream Boundary Conditions

River temperature responded differently to perturbations of dam discharge volume and temperature when aggregating results into periods of seasonal cooling versus warming, but discharge temperature often had a larger effect compared to discharge volume (Figure 8). During the cooling period (November–January) river temperature tends to decrease in a downstream direction. In this period, changing the discharge volume of Keswick Dam had little effect on downstream river temperature (nearly horizontal isoline on each of the three river reaches indicating that as dam discharge volume changes downstream temperature varies

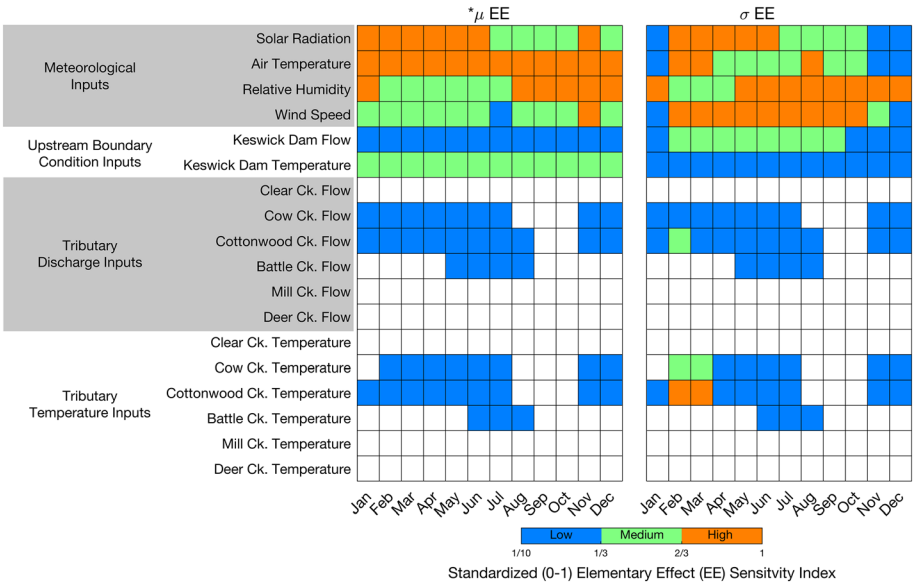

Figure 6. Temporally explicit sensitivity index from the elementary effects test scaled (0–1) for each of the 18 inputs explored, with 12 retained, in the screening sensitivity analysis and categorized, based on the scaled elementary effects test values as having low (value >1/10–1/3), medium (value >1/3 to 2/3), or high sensitivity (value >2/3) to a given input. White cells are inputs not categorized (i.e., value of ≤1/10) and were inferred to have a negligible effect on model output. Note that, for tributary inputs, creeks are ordered from upstream to downstream.

only slightly, Figure 8a). During the warming period (February–October), the effect of release temperature and discharge varied by reach. Reach-1 river temperature responded primarily to changes in discharge temperature (Figure 8b upper plot, nearly horizontal isolines), with the exception of flows below 150 cms. In contrast, in Reach-3 more than half of the simulation space had river temperatures responding most strongly to dam discharge volume or both discharge volume and temperature. For results stratified by month, see supporting information Figure S7.

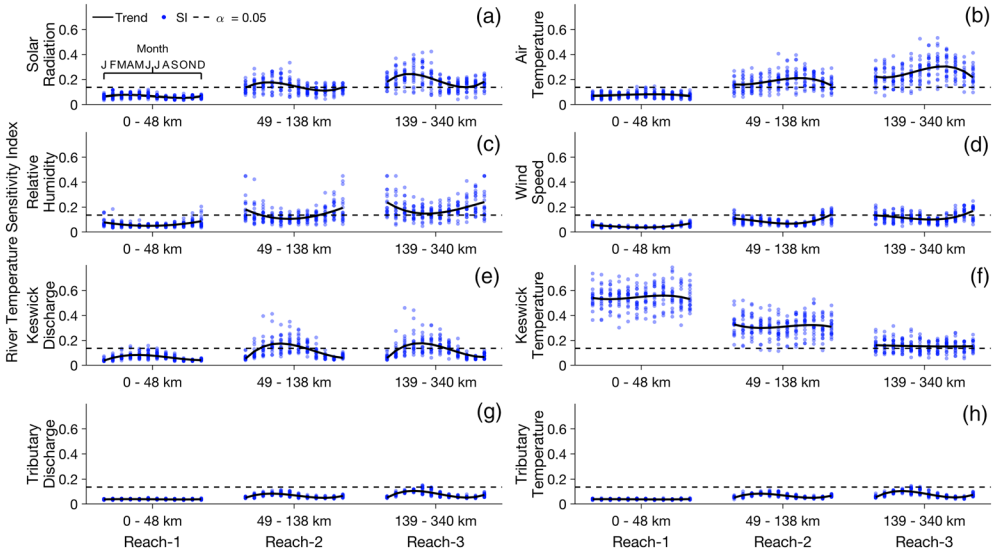

Figure 7. Sacramento River water temperature sensitivity indices from PAWN analysis stratified by month and river reach. PAWN sensitivity indices range from 0–1, with higher values corresponding to greater river temperature sensitivity to a given model input. Each month is comprised of 50 conditioning points (blue dot) for each input (i.e., PAWN parameter $n = 50$), with a general trend for each reach and input from a polynomial model (black line). Also displayed is the critical value (α) of the KS test statistic with confidence of 0.05 (dashed line).

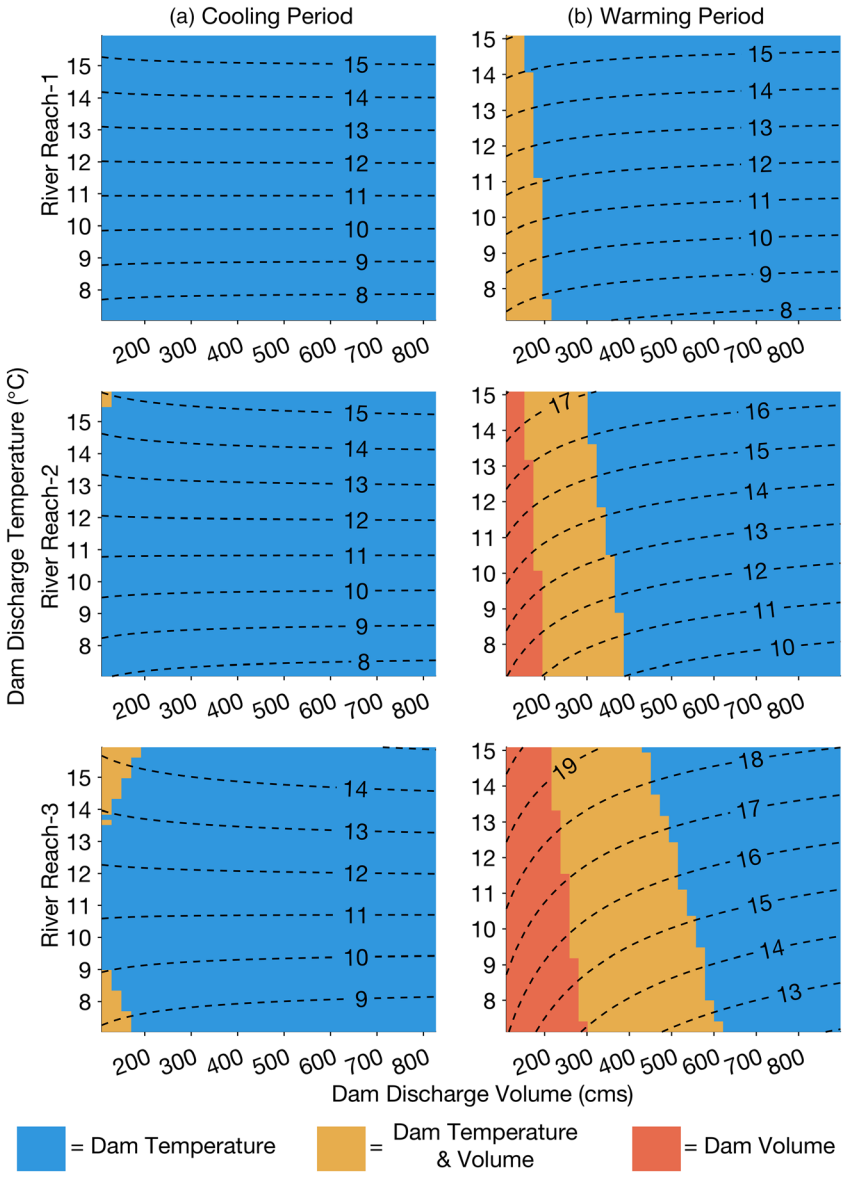

Figure 8. Classification of the river temperature response to perturbations of either dam discharge volume (*X* axis) or dam discharge temperature (*Y* axis). Rows show the three reaches of the Sacramento River, during cooling (a; November–January) and warming (b; February–October) periods. The primary upstream driver of temperature change (see Figure 3) is color coded (dam temperature: blue dot; volume: red dot; both temperature and volume: orange dot). Isolines represent constant output of mean monthly temperature within the input space of discharge volume and temperature (dashed line).

4. Discussion

We used a mechanistic river temperature model combined with global sensitivity analysis to characterize spatial and temporal variability in river temperature, heat flux, and the drivers of temperature change in a large regulated river. Heat flux had the greatest magnitude and variability in river sections closest to the dam. The primary drivers of river temperature were more variable spatially than temporally and were dominated by meteorological forcings (i.e., air temperature and solar radiation) and upstream boundary conditions (i.e., dam discharge temperature), and less sensitive to tributary inputs. For the upstream boundary conditions, dam discharge temperature, more often than discharge volume, was a primary factor controlling Sacramento River temperature. These results highlight the spatial variability in drivers of river temperature,

and the importance of upstream boundary conditions (i.e., as a result of reservoirs and dam operations) on downstream aquatic habitat.

While the boundary conditions of temperature and discharge volume fundamentally set the rate of heat flux that will occur downstream, the relative importance of these two inputs has not been well demonstrated to date. Most studies on reservoir and dam impacts on river temperature focus on discharge volume (Prats et al., 2012; Preece & Jones, 2002; Van Vliet et al., 2011) or compare predam and postdam impacts on river temperature (Cai et al., 2018). We estimated that for much of the year Sacramento River's temperature would respond more strongly to changes in upstream discharge temperature than to discharge volume. These findings highlight the importance of travel time in a river system when release temperature from a dam is not at or near equilibrium with atmospheric conditions, as it represents the duration of time a parcel of water is exposed to warming and/or cooling processes and forced toward temperature equilibrium (i.e., the river temperature at which heat exchange is 0). For the Sacramento River, travel time associated with Reach-1 is on average less than 24 hr, while travel time for Reach-3 is often greater than 5 days. The relatively short travel time in Reach-1 results in a parcel of water released from Keswick Dam having little time to change from its initial release temperature toward the equilibrium temperature. This same parcel of water has much more time to be forced toward equilibrium while traveling to Reach-3. When discharge volume did dominate the response, it did so farthest from the upstream boundary in Reach-3, at low discharge (<200 cms, which occurs ~30% of the time), and during February through October, when the Sacramento River tended to warm as it moved downstream. This finding can be related to the variability in travel time. Under the simulated discharge volume (Figure 8) travel time in Reach-1 ranged from 14 to 30 hr, while Reach-3 ranged from 4 to 7 days. The larger variability in Reach-3 results in changes to discharge volume in that reach having larger cumulative effects on river temperature dynamics and thus greater river temperature sensitivity.

Air temperature and solar radiation are important drivers of river temperature (Kaushal et al., 2010; Roth et al., 2010), but their spatial influence has not been well quantified. Our results provide novel evidence of strong longitudinal variation in the sensitivity of river temperature to air temperature and solar radiation, despite there being little variation in these meteorological forcing terms between reaches (see supporting information Figure S8). Sacramento River temperature was observed to be weakly sensitive to the variability in these inputs in Reach-1 and strongly sensitive to them in Reach-3. The difference in sensitivity across space can be attributed to the cumulative energy inputs from air temperature and solar radiation as water and heat is advected downstream: the overall impact on a water parcel's temperature budget accumulates with distance downstream and thus becomes more sensitive to background meteorological variability. This finding broadly relates to how a river responds to temperature shifts and suggests that increases/decreases in diffuse heat sources will have a greater effect on river temperature dynamics further downstream from upstream boundary conditions, for example, dams or headwater springs.

In general, there was some level of monthly variation in the sensitivity of river temperature to most inputs. There was a high level of temporal sensitivity to solar radiation, particularly from February to June, when variation in cloud cover is largest in our study region (see Figure 2). Temporal sensitivity was also highest for relative humidity from November to February when humidity is often the closer to saturation and suggests that time periods when latent heat of evaporation is reduced can have important controls on river temperature dynamics. These results highlight the inferential ability gained in our study by basing input perturbations on observed monthly temporal variability instead of applying identical perturbations across all months, for example, perturb values by ±10% from a mean value. Sensitivity analysis, by definition, is in reference to the range of input values considered. Because we based our perturbations on monthly historical conditions, our results are framed in this context. Put another way, our analysis provided monthly level insights into the sensitivity of river temperature to meteorology, hydrology, and dam discharge conditions using historical variability as the baseline. Related research into the importance of conducting time-varying sensitivity analysis to explore performance of hydrologic models has also documented the benefit of disaggregating time (Pianosi & Wagener, 2016).

While tributary inputs have been documented to alter mainstem temperatures and/or provide localized areas of temperature heterogeneity in other river systems (Ebersole et al., 2014; Monk et al., 2013), they do little to change the mainstem temperature over the reach scales examined in our study. To further explore this finding, we conducted post hoc analysis (Figure 9) on Cow Creek during the month of May, a tributary

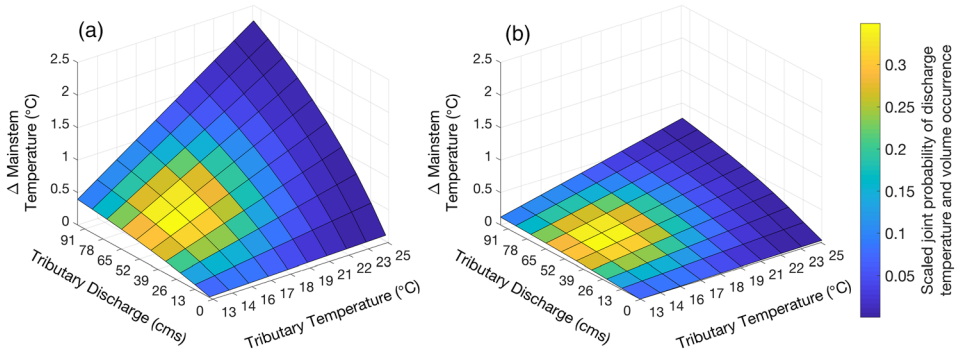

Figure 9. Simulated change in mainstem temperature of the Sacramento River (*Z* axis) over a suite of historical inflow volumes (*Y* axis) and temperatures (*X* axis) of Cow Creek during the month of May. Joint probabilities of a flow and temperature combinations are color coded. Note that two spatial scales are displayed, (a) for the model segment where the tributary enters (2 km length) and (b) for the entire reach where the tributary enters (48 km length; Reach-1 in Figure 1).

and time period for which our results indicated had one of the greater impacts on mainstem temperature (data not shown). The analysis consisted of running a suite of RAFT simulations over historic Cow Creek inflow volumes and temperatures and then evaluating how these changed mainstem temperature at the model segment (Figure 9a) and reach (Figure 9b) where Cow Creek enters the Sacramento River. From this analysis, we observed two reasons why river temperature was largely insensitive to tributary inputs in our study. First, primarily related to our analytical approach, tributaries function as point source inputs to rivers and our sensitivity analysis (conducted at a reach-scale) dampened the effect of localized, lateral, and inputs. This is demonstrated in Figure 9, where the model segment where Cow Creek enters the mainstem (a) had a much higher temperature response (*X* axis) for a given Cow Creek discharge volume and temperature pair compared to the reach where the tributary enters (b). This finding indicates that our reach-scale analysis may not be well suited to identify model sensitivity for lateral point source loadings from tributaries at subreach scales. Second and more broadly general to river systems as a whole, large volumes of tributary input at temperatures colder or warmer than the receiving river are required to impact mainstem temperatures. The probability of warm high flows necessary to impact the cold river temperatures of the Sacramento in May are rare (Figure 9, color schema). Under typical tributary volumes and temperatures Cow Creek was estimated to raise Sacramento River temperature by <0.5 °C.

While our study accounted for primary factors affecting river temperature dynamics, we did not include all potential drivers of temperature change. For example, riparian and topographic shading and hyporheic/groundwater exchange rates have been observed to impact river temperature dynamics in some systems (Arrigoni et al., 2008; Garner et al., 2014). Studies that have found significant effects of channel shading are often done on systems with smaller channel widths (Garner et al., 2017; Johnson & Jones, 2000; Wondzell et al., 2019), while studies on river widths greater than 100 m, like the Sacramento River (Michalková et al., 2011), found lower effects of shading (DeWalle, 2008). Likewise, most studies of hyporheic and or groundwater exchange occur on smaller discharge systems where instrumentation can be used to estimate rates of water exchange between the bed and channel (Bhaskar et al., 2012; Snyder et al., 2015). While we simulated heat exchange and the water-bed interface, we did not perturb this factor in our sensitivity analysis. For the Sacramento River, which rarely has a discharge value less than 140 cms, and in other large discharge river systems, empirically measuring the effects of hyporheic flows to parameterize a water temperature model would be challenging but should nevertheless be considered for future research.

While this study used a particular research method on a single river system, global sensitivity analysis on the Sacramento River, these finding are applicable to other river systems with similar qualities and these analysis methods can be used elsewhere to infer drivers of river temperature. For example, like the Sacramento River, currently over 63% of larger rivers (i.e. > 1,000 km in length) are damned worldwide and have aquatic fauna/habitat downstream that may be impacted by shifts in river temperatures (Grill et al., 2019).

Understanding how a particular system is impacted by upstream inputs (i.e., dams and reservoirs) as well a local meteorology and other forcing conditions is valuable information for resource management and planning. The method we have outlined in this work (i.e., global sensitivity analysis bounded by historical conditions) provides a framework to attain such information and is adaptable to other river systems.

In conclusion, both dam operations and meteorological conditions have important, spatially and temporally variable influences on river temperature. The management implications of these findings are significant as they relate to downstream thermal habitat. Within the context of the historical variability of river temperature drivers, we found dam discharge temperature to provide greater scope for management of river temperature than discharge volume, although volume became important under summer low-flow conditions in locations further from the dam. While dam operations (discharge volume and in some cases temperature) can be directly managed, the amount of downstream habitat that can be influenced by dam operations is dependent on upstream conditions, such as reservoir storage capacity and a dam's selective withdrawal capabilities (i.e., ability to withdraw water from various elevations in a reservoir). While our results highlight the importance of boundary conditions (i.e., the effect of dams) as a primary driver of downstream river temperature, future work evaluating the ability to sustain downstream temperature control under varying reservoir and dam operational conditions, and meteorological conditions, is needed to better understand the utility of upstream boundary conditions to control downstream temperatures.

Acknowledgments
This research was supported by funding from the U.S. Bureau of Reclamation. Early development of the manuscript benefited from discussions with Vamsi Krishna Sridharan. David Boughton provided valuable edits and suggestions during internal review. Primary model output used for analysis is available for download online (https://oceanview.pfeg.noaa.gov/CVTEMP/download).

References

Angilletta, M. J. Jr., & Angilletta, M. J. (2009). *Thermal adaptation: A theoretical and empirical synthesis*. Oxford: Oxford University Press.

Arrigoni, A. S., Poole, G. C., Mertes, L. A., O'Daniel, S. J., Woessner, W. W., & Thomas, S. A. (2008). Buffered, lagged, or cooled? Disentangling hyporheic influences on temperature cycles in stream channels. *Water Resources Research*, *44*, W09418. https://doi.org/10.1029/2007WR006480

Bhaskar, A. S., Harvey, J. W., & Henry, E. J. (2012). Resolving hyporheic and groundwater components of streambed water flux using heat as a tracer. *Water Resources Research*, *48*, W08524. https://doi.org/10.1029/2011WR011784

Boulêtreau, S., Salvo, E., Lyautey, E., Mastrorillo, S., & Garabetian, F. (2012). Temperature dependence of denitrification in phototrophic river biofilms. *Science of the Total Environment*, *416*, 323–328. https://doi.org/10.1016/j.scitotenv.2011.11.066

Cai, H., Piccolroaz, S., Huang, J., Liu, Z., Liu, F., & Toffolon, M. (2018). Quantifying the impact of the Three Gorges Dam on the thermal dynamics of the Yangtze River. *Environmental Research Letters*, *13*(5), 054016.

Caissie, D. (2006). The thermal regime of rivers: A review. *Freshwater Biology*, *51*(8), 1389–1406.

Campolongo, F., Cariboni, J., & Saltelli, A. (2007). An effective screening design for sensitivity analysis of large models. *Environmental Modelling & Software*, *22*(10), 1509–1518.

Chapra, S. C. (2008). *Surface water-quality modeling*. Long Grove IL: Waveland Press.

Chen, J., Brissette, F. P., Chaumont, D., & Braun, M. (2013). Performance and uncertainty evaluation of empirical downscaling methods in quantifying the climate change impacts on hydrology over two North American river basins. *Journal of Hydrology*, *479*, 200–214.

Costard, F., Dupeyrat, L., Gautier, E., & Carey-Gailhardis, E. (2003). Fluvial thermal erosion investigations along a rapidly eroding river bank: Application to the Lena River (central Siberia). *Earth Surface Processes and Landforms: The Journal of the British Geomorphological Research Group*, *28*(12), 1349–1359.

Demars, B. O., Russell Manson, J., Olafsson, J. S., Gislason, G. M., Gudmundsdottír, R., Woodward, G., et al. (2011). Temperature and the metabolic balance of streams. *Freshwater Biology*, *56*(6), 1106–1121.

DeWalle, D. R. (2008). Guidelines for riparian vegetative shade restoration based upon a theoretical shaded-stream model 1. *JAWRA Journal of the American Water Resources Association*, *44*(6), 1373–1387.

Ebersole, J. L., Wigington, P. J. Jr., Leibowitz, S. G., Comeleo, R. L., & Sickle, J. V. (2014). Predicting the occurrence of cold-water patches at intermittent and ephemeral tributary confluences with warm rivers. *Freshwater Science*, *34*(1), 111–124.

Elsner, J. B., & Tsonis, A. A. (2013). *Singular spectrum analysis: A new tool in time series analysis*. Berlin: Springer Science & Business Media.

Evensen, G. (2009). *Data assimilation: The ensemble Kalman filter*. Berlin: Springer Science & Business Media.

Garner, G., Malcolm, I. A., Sadler, J., & Hannah, D. (2014). What causes cooling water temperature gradients in a forested stream reach? *Hydrology and Earth System Sciences*, *18*(12), 5361–5376.

Garner, G., Malcolm, I. A., Sadler, J. P., & Hannah, D. M. (2017). The role of riparian vegetation density, channel orientation and water velocity in determining river temperature dynamics. *Journal of Hydrology*, *553*, 471–485.

Grill, G., Lehner, B., Thieme, M., Geenen, B., Tickner, D., Antonelli, F., et al. (2019). Mapping the world's free-flowing rivers. *Nature*, *569*(7755), 215–221. https://doi.org/10.1038/s41586-019-1111-9

Hogg, R. V., Tanis, E. A., & Zimmerman, D. L. (1977). *Probability and statistical inference*. New York: Macmillan.

Johnson, S. L., & Jones, J. A. (2000). Stream temperature responses to forest harvest and debris flows in western Cascades, Oregon. *Canadian Journal of Fisheries and Aquatic Sciences*, *57*(S2), 30–39.

Kaushal, S. S., Likens, G. E., Jaworski, N. A., Pace, M. L., Sides, A. M., Seekell, D., et al. (2010). Rising stream and river temperatures in the United States. *Frontiers in Ecology and the Environment*, *8*(9), 461–466.

Martins, E. G., Hinch, S. G., Patterson, D. A., Hague, M. J., Cooke, S. J., Miller, K. M., et al. (2011). Effects of river temperature and climate warming on stock-specific survival of adult migrating Fraser River sockeye salmon (*Oncorhynchus nerka*). *Global Change Biology*, *17*(1), 99–114.

Michalková, M., Piégay, H., Kondolf, G., & Greco, S. (2011). Lateral erosion of the Sacramento River, California (1942–1999), and responses of channel and floodplain lake to human influences. *Earth Surface Processes and Landforms*, *36*(2), 257–272.

Monk, W. A., Wilbur, N. M., Curry, R. A., Gagnon, R., & Faux, R. N. (2013). Linking landscape variables to cold water refugia in rivers. *Journal of Environmental Management*, *118*, 170–176.

Morris, M. D. (1991). Factorial sampling plans for preliminary computational experiments. *Technometrics*, *33*(2), 161–174.
NARR (2004). North American Regional Reanalysis: A long-term, consistent, high-resolution climate dataset for the North American domain, as a major improvement upon the earlier global reanalysis datasets in both resolution and accuracy, Fedor Mesinger et. al, submitted to BAMS 2004.
Niemeyer, R. J., Cheng, Y., Mao, Y., Yearsley, J. R., & Nijssen, B. (2018). A thermally stratified reservoir module for large-scale distributed stream temperature models with application in the Tennessee River basin. *Water Resources Research*, *54*, 8103–8119. https://doi.org/10.1029/2018WR022615
Norton, G. E., & Bradford, A. (2009). Comparison of two stream temperature models and evaluation of potential management alternatives for the Speed River, Southern Ontario. *Journal of Environmental Management*, *90*(2), 866–878. https://doi.org/10.1016/j.jenvman.2008.02.002
Null, S. E., Deas, M. L., & Lund, J. R. (2010). Flow and water temperature simulation for habitat restoration in the Shasta River, California. *River Research and Applications*, *26*(6), 663–681.
Olden, J. D., & Naiman, R. J. (2010). Incorporating thermal regimes into environmental flows assessments: Modifying dam operations to restore freshwater ecosystem integrity. *Freshwater Biology*, *55*(1), 86–107.
Pianosi, F., Beven, K., Freer, J., Hall, J. W., Rougier, J., Stephenson, D. B., & Wagener, T. (2016). Sensitivity analysis of environmental models: A systematic review with practical workflow. *Environmental Modelling & Software*, *79*, 214–232.
Pianosi, F., & Wagener, T. (2015). A simple and efficient method for global sensitivity analysis based on cumulative distribution functions. *Environmental Modelling & Software*, *67*, 1–11.
Pianosi, F., & Wagener, T. (2016). Understanding the time-varying importance of different uncertainty sources in hydrological modelling using global sensitivity analysis. *Hydrological Processes*, *30*(22), 3991–4003.
Pike, A., Danner, E., Boughton, D., Melton, F., Nemani, R., Rajagopalan, B., & Lindley, S. (2013). Forecasting river temperatures in real time using a stochastic dynamics approach. *Water Resources Research*, *49*, 5168–5182. https://doi.org/10.1002/wrcr.20389
Poole, G. C., & Berman, C. H. (2001). An ecological perspective on in-stream temperature: Natural heat dynamics and mechanisms of human-caused thermal degradation. *Environmental Management*, *27*(6), 787–802. https://doi.org/10.1007/s002670010188
Prats, J., Val, R., Dolz, J., & Armengol, J. (2012). Water temperature modeling in the lower Ebro River (Spain): Heat fluxes, equilibrium temperature, and magnitude of alteration caused by reservoirs and thermal effluent. *Water Resources Research*, *48*, W05523. https://doi.org/10.1029/2011WR010379
Preece, R. M., & Jones, H. A. (2002). The effect of Keepit Dam on the temperature regime of the Namoi River, Australia. *River Research and Applications*, *18*(4), 397–414.
Roth, T., Westhoff, M., Huwald, H., Huff, J., Rubin, J., Barrenetxea, G., et al. (2010). Stream temperature response to three riparian vegetation scenarios by use of a distributed temperature validated model. *Environmental Science & Technology*, *44*(6), 2072–2078. https://doi.org/10.1021/es902654f
Saltelli, A., Ratto, M., Andres, T., Campolongo, F., Cariboni, J., Gatelli, D., et al. (2008). *Global sensitivity analysis: The primer*. Hoboken, NJ: John Wiley & Sons.
Snyder, C. D., Hitt, N. P., & Young, J. A. (2015). Accounting for groundwater in stream fish thermal habitat responses to climate change. *Ecological Applications*, *25*(5), 1397–1419. https://doi.org/10.1890/14-1354.1
Toffolon, M., & Piccolroaz, S. (2015). A hybrid model for river water temperature as a function of air temperature and discharge. *Environmental Research Letters*, *10*(11).
Van Vliet, M., Ludwig, F., Zwolsman, J., Weedon, G., & Kabat, P. (2011). Global river temperatures and sensitivity to atmospheric warming and changes in river flow. *Water Resources Research*, *47*, W02544. https://doi.org/10.1029/2010WR009198
Webb, B., & Zhang, Y. (1997). Spatial and seasonal variability in the components of the river heat budget. *Hydrological Processes*, *11*(1), 79–101.
Wondzell, S. M., Diabat, M., & Haggerty, R. (2019). What matters most: Are future stream temperatures more sensitive to changing air temperatures, discharge, or riparian vegetation? *JAWRA Journal of the American Water Resources Association*, *55*(1), 116–132.
Yearsley, J. (2012). A grid-based approach for simulating stream temperature. *Water Resources Research*, *48*, W03506. https://doi.org/10.1029/2011WR011515